Multi-layer Piezoelectric Energy Harvesters for Improved Power Generation

S. Rammohan[a], Sanketh Chiplunkar[c], C. M. Ramya[c], S. Jayanth Kumar [b], Anjana Jain[b], Rudra Pratap[a,c]

[a] Department of Mechanical Engineering, Indian Institute of Science, Bangalore 560012
[b] National Aerospace Laboratories, Bangalore 560017
[c]Centre for Nano Science and Engineering, Indian Institute of Science, Bangalore 560012
Email: rammohan@mecheng.iisc.ernet.in

Abstract: Low power consuming sensor networks have drawn the attention of many researchers in the domain of energy harvesting using smart materials. Piezoelectric smart materials have been extensively studied to transform the mechanical energy in the form of vibrations to electrical energy. There have been several attempts to improve the generated power by optimizing the harvester configuration and the processing electronics. In this paper, a multi-layer configuration of a cantilever based harvester is analyzed and compared with a bimorph configuration. Published models of bimorphs assume that the piezoelectric material covers the cantilever completely. This paper focuses on studying the partial coverage of piezoelectric material on the beam and analyzing the multi-layer configuration of the active material. It is observed analytically and experimentally that the multi-layer configuration is superior to the bimorphs when compared for the same volume of the piezoelectric material used. Experimentally, multilayer harvester and bimorphs made of Polyvinylidinefluoride (PVDF) are tested under similar conditions to observe that the multilayer harvester generates 230 $\mu W/cm^3/g^2$ which is more than twice the value obtained from bimorphs, thus demonstrating a better than 100% improvement in performance.

Keywords: Energy harvesting, PVDF bimorphs, multilayers harvesters, electro-structural coupling coefficient, optimal load resistance.

1. INTRODUCTION

The development of ultra-low power consuming sensor nodes has stimulated tremendous interest in harvesting energy from the ambience. Energy harvesting refers to tapping that portion of easily available energy which is not the primarily intended form of the system's energy. Hence, the magnitude of harvestable and harvested energy depends on the system under consideration. Nevertheless, even limited amounts of harvested energy combined with ultra-low power consuming electronics open up plethora of avenues in remote sensing networks and structural health monitoring. Electrostatic, electromagnetic, piezoelectric and tribo-electric effects are some of the notable mechanisms of converting mechanical energy into electrical energy. Power densities in piezoelectric mechanism are comparable with those in electromagnetic mechanism[1]. Moreover, piezoelectric mechanism is perhaps the best suited to harvest energy from vibrations at low frequencies[2].

The conversion of energy from one form to another is the key function of *smart* materials which is the basis for energy harvesting. Over the years, researchers have been analyzing piezoelectric materials for energy harvesting. The most common form of a harvester in the form of a cantilever is either a unimorph or a bimorph. Bimorphs have two layers of piezoelectric material on either side of the substrate. These bimorphs exchange energy between mechanical and electrical domains owing to the cross coupling between the directions of stress and polarization. Depending on the poling direction in each layer of piezoelectric material, layer terminals can be combined either in series or parallel[3]. Improvement in the energy generated from the harvester is achieved by optimizing the configuration and/or processing electronics. The focus in the recent years has been on improving the switching circuits for piezoelectric harvesting[4,5]. The present work lays emphasis on improving the performance of the harvester through multi-layered configuration. Most published designs assume that the piezoelectric material is covered completely on the beam[6]. There are certain approximate designs which model the partial coverage as pin force model or an equivalent beam model[7,8]. The current work discusses the method of analyzing partial coverage on the beam with no approximations. Section 2 elaborates the method followed in analyzing stepped beam using extended Hamilton's principle. This generic design is further extended to model the multi-layer configuration of the harvester. Simulation and experimental results from a PVDF multi-layer harvester are presented and compared. Despite the weak coupling observed in PVDF, the normalized power densities improve significantly in multi-layer configuration when compared to the bimorph configuration. Finally, the advantages of multi-layer harvesters over the bimorph configuration are discussed to show that even low profile piezoelectric materials which have weak coupling can result in enhanced levels of power generation through appropriate design.

2. GENERIC DESIGN OF PIEZOELECTRIC STEPPED BEAM

A piezoelectric structure is associated with electrical, thermal and mechanical energies. Equations of motion for a stepped beam with a piezoelectric layer are derived using the extended Hamilton's principle. This principle, originally used to analyze piezoelectric actuators, is employed by many researchers to describe the behavior of a bimorph[9]. The derivation of equations of motion of the harvester, in a generic configuration (Figure 1) with partial coverage of

piezoelectric material and an end mass is described in this section. The first variation of action integral A in the case of an elastic dielectric using extended Hamilton's principle is written as follows,

$$\delta A = \int_{t_1}^{t_2} \left(\delta K - \delta U + \delta W_e + \delta W_{nc} \right) dt = 0 \tag{1}$$

where, K is the kinetic energy, U the strain energy, W_e is the electrical energy and W_{nc} is the non-conservative work. The linear isothermal constitutive relations for a piezoelectric beam, under the assumption that all strains and electric fields except longitudinal strain S_1 and electric field across thickness E_3 vanish, are given as follows,

$$\begin{aligned} T_1 &= c_{11} S_1 - e_{31} E_3 \\ D_3 &= e_{31} S_1 + \varepsilon_{33} E_3 \end{aligned} \tag{2}$$

where, T1 is the longitudinal stress and D_3 is the electric displacement in thickness direction, c_{11}, e_{31} and ε_{33} are elastic modulus, piezoelectric stress coefficient and relative permittivity, respectively. Using Euler Bernoulli hypothesis for thin beams and writing the transverse displacement of the beam as $w(x,t)$, the strain in the beam at a height of interest z is given by equation (3), where $\bar{z}$ is the height of the neutral surface. A composite beam made of two materials has neutral surface at a height given by equation (4), where c indicates the elastic modulus, A is the cross sectional area, t is the thickness and the subscripts denote the material indices in equations (4) and (5).

$$S_1 = -\left(z - \bar{z} \right) w_{,xx} \tag{3}$$

$$\bar{z} = \frac{c_1 A_1 \left(\frac{t_1}{2} \right) + c_2 A_2 \left(t_1 + \frac{t_2}{2} \right)}{c_1 A_1 + c_2 A_2} \tag{4}$$

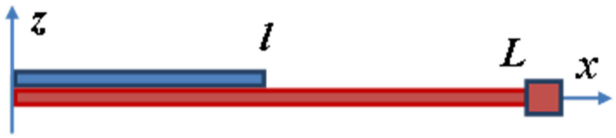

Figure 1. Schematic of a stepped beam of length L and end mass with piezoelectric strip coverage length l.

Following appropriate sign conventions for bending moment and beam curvature, the equivalent flexural rigidity for the composite beam is derived and is given by equation (5), where I_1, I_2 represent the respective moments of inertia of the cross sectional areas.

$$EI_{eqv} = c_1 I_1 + c_2 I_2 + \frac{c_1 I_1 c_2 I_2}{c_1 I_1 + c_2 I_2} \left(\frac{t_1 + t_2}{2} \right)^2 \tag{5}$$

Employing the relations given in equations (2) through (5), the first variation of the action integral in equation (1) requires variations to be taken on two variables, namely, transverse displacement $w(x,t)$ and electric potential $V(t)$. Let L denote the total length of the beam and l the length of the piezoelectric strip. Expressing the transverse displacement in variable separable form as a product of spatial function $\Phi_1(x)$ in segment 1 and $\Phi_2(x)$ in segment 2, and the temporal function W(t), the boundary terms are described below,

$$\phi_1 \big|_{x=l} = \phi_2 \big|_{x=l} \; ; \quad \phi_{1,x} \big|_{x=l} = \phi_{2,x} \big|_{x=l} \tag{6}$$

$$\begin{aligned} EI_{eq1} \phi_{1,xx} \big|_{x=l} &= EI_{eq2} \phi_{2,xx} \big|_{x=l} \\ EI_{eq1} \phi_{1,xxx} \big|_{x=l} &= EI_{eq2} \phi_{2,xxx} \big|_{x=l} \end{aligned} \tag{7}$$

$$\begin{aligned} m_t \phi_2 \big|_{x=L} W_{,tt} - EI_{eq2} W \phi_{2,xxx} \big|_{x=L} &= 0 \\ J \phi_{2,x} \big|_{x=L} W_{,tt} + EI_{eq2} W \phi_{2,xx} \big|_{x=L} &= 0 \end{aligned} \tag{8}$$

Equations (6) ensure the displacement and slope continuity at the step. Shear force and bending moment continuity at the step are described by equations (7). End mass m_t with polar moment of inertia J at the beam tip contributes to the shear and moment expressed in equations (8). After screening out the boundary terms from equation (1) the variations on displacement and voltage result in the equations of motion in weak form as follows:

$$\begin{aligned} MW_{,tt} + CW_{,t} + KW - GV &= F \\ RC_p V_{,t} + RGW_{,t} + V &= 0 \end{aligned} \tag{9}$$

where,

$$\begin{aligned} M &= \int_0^l \bar{m}_1 \phi_1^2 dx + \int_l^L \bar{m}_2 \phi_2^2 dx + m_t \phi_2^2 \big|_{x=L} + J \phi_{2,x}^2 \big|_{x=L} \\ C &= \int_0^l r_1 \phi_1^2 dx + \int_l^L r_2 \phi_2^2 dx \\ K &= \int_0^l EI_{eq1} \phi_{1,xx}^2 dx + \int_l^L EI_{eq2} \phi_{2,xx}^2 dx \\ G &= b_1 e_{31} \left(\frac{t_1}{2} - \bar{z} \right) \phi_{1,x} \big|^{x=l} \\ F &= -\int_0^l \bar{m}_1 \phi_1 w_{g,tt} dx - \int_l^L \bar{m}_2 \phi_2 w_{g,tt} dx - m_t w_{g,tt} \phi_2 \big|_{x=L} - J \alpha \phi_{2,x} \big|_{x=L} \\ C_p &= \frac{b_1 l \varepsilon_{33}}{t_1} \end{aligned} \tag{10}$$

The coefficients in equation (9) depend on the shape functions, mass per unit length $\bar{m}$, velocity independent coefficient of friction r, in the two segments of the beam and ground displacement w_g, base angular acceleration α, piezoelectric beam width b_1, and thickness t_1. R represents the load resistance across which the power from the harvester is measured.

3. DESIGN OF MULTI-LAYERED PIEZOELECTRIC BEAM

The generic formulation described above holds even with multi-layered harvester except for modifications described in this section. Let a segment of the beam be covered by n layers of piezoelectric films as shown in Figure 2. The height of the neutral surface is derived assuming the elemental beam to be in pure bending consistent with the sign conventions followed in the earlier derivations, and is given by

$$\bar{z} = \frac{\sum_{i=1}^{n} c_i A_i \sum_{j=1}^{i} t_j - \sum_{i=1}^{n} c_i A_i \frac{t_i}{2}}{\sum_{i=1}^{n} c_i A_i} \tag{11}$$

Besides, the equivalent flexural rigidity for the segment of the beam covered with several piezoelectric layers is derived conforming to the stress and bending moment sign conventions as follows:

$$EI_{eq} = \sum_{i}^{n} b_i c_i \left(t_i \left(\sum_{j=1}^{i} t_j - \bar{z} \right) \left(\sum_{j=1}^{i-1} t_j - \bar{z} \right) + \frac{t_i^3}{3} \right) \tag{12}$$

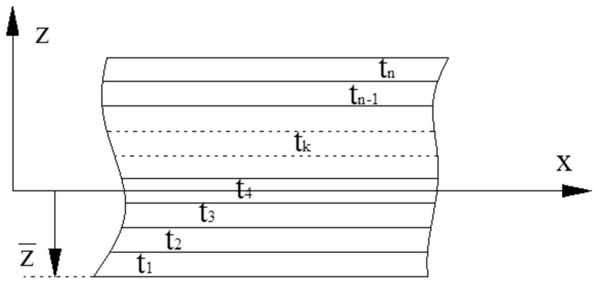

Figure 2. Elemental length of multi-layer piezoelectric beam showing thicknesses of each layer and the position of the neutral axis.

It can be noted that the relations in equations (11) and (12) are in close agreement with those derived in reference [10]. The performance improvement associated with the multilayer harvester is partly bestowed in the enhancement of the electro-structural coupling coefficient *G*, and the total capacitance C_p. The boundary terms described in equations (6) through (8) and the equations of motion in equation (9) hold even in the multi-layer harvester except for the following two changes.

$$G = \sum_{i=1}^{n} b_i e_{31i} \left(\left(\sum_{j=1}^{i} t_j - \bar{z} \right) - \frac{t_i}{2} \right) \phi_{1,x} \Big|^{x=l} \tag{13}$$

$$C_p = \sum_{i=1}^{n} \frac{b_i l \varepsilon_{33}}{t_i} \tag{14}$$

The shape functions satisfying the boundary conditions in (6) and (7), for the first mode of vibration, with no end mass are described by the following two equations,

$$\phi_1(x) = \frac{2EI_{eq2}\left(3(L+l)-2x\right)x^2}{3EI_{eq1}(L-l)^3 + 2EI_{eq2}l\left(l^2-3lL+6L^2\right)} \tag{15}$$

The shape function in equation (15) does not have lower order terms in x due to the clamped boundary condition on one end. These shape functions can also be easily derived for the stepped beam including the tip mass but are not shown here for brevity. Using the shape functions for the multi-layer harvester and the equations of motion (9) and (10), the tip displacement, *W,* and the electrical potential, *V*, are solved for harmonic base excitation. The power developed by the harvester is computed using r.m.s value of the voltage across the load resistance, *R*, as follows:

$$P = \frac{V^2}{2R} \tag{17}$$

For the given parameters of the harvester as in equation (10), there exists an optimum value of load resistance at which the power delivered is maximum. Differentiating the power given in equation (17) and rearranging, the optimum load resistance is given as

$$R_{opt} = \frac{1}{i\omega\left\{C_p + \dfrac{G^2}{\left(K - M\omega^2 + iC\omega\right)}\right\}} \tag{18}$$

It can be assimilated from the above equation that when G is insignificant, the optimum load resistance is governed only by ωC_p, where ω is the excitation frequency, but as G increases, optimum resistance keeps reducing which is noticed in multi-layered harvester and is discussed at length in the next section. Substituting R_{opt} from equation (18) for *R* into equation (17), the peak power generated by the harvester can be obtained.

4. SIMULATIONS AND EXPERIMENTS

The performance of harvester in two configurations – bimorph and multiple layers of PVDF is simulated and experimentally verified. A multi-layer harvester is fabricated using 60 μm thick PVDF film and a 100 μm thick copper substrate. Three layers are bonded on either sides of the Cu substrate. All the six layers are placed in such a way that during bending, every layer contributes additively to the generated power. The length of the copper beam is 40 mm and that of the PVDF film is 25 mm from the fixed end. A tip mass of 0.63 gm is attached to the free end of the beam, however, the rotary inertia of the mass is neglected in simulations.

The beam resonance is estimated by solving the characteristic equation obtained by assuming transcendental form of shape functions in the two segments. In order to validate the proposed model for stepped beam, piezoelectric layers are laid to cover partially the copper substrate. The dependence of potential on load resistance is simulated and measured. Subsequently, the optimum load resistance given by equation (18) for the harvester is verified experimentally. Furthermore, the model is validated by measuring the layer-wise potential and comparing it with the simulated values across several load resistances. Tip deflection of the beam is simulated for an input vibration of 0.5 g across load resistances from 0.5 to 2 MΩ. The variation in the deflection with frequency and resistance is shown in Figure 3. The maximum deflection occurs at the beam resonance which is 30 Hz.

$$\phi_2(x) = \frac{2EI_{eq2}l(L-l)\left(l^2-3lL+6Lx\right) + EI_{eq1}\left(3l^2-8lL+6L^2+2(l-2L)x+x^2\right)(l-x)^2}{(L-l)\left(3EI_{eq1}(L-l)^3 + 2EI_{eq2}l\left(l^2-3lL+6L^2\right)\right)} \tag{16}$$

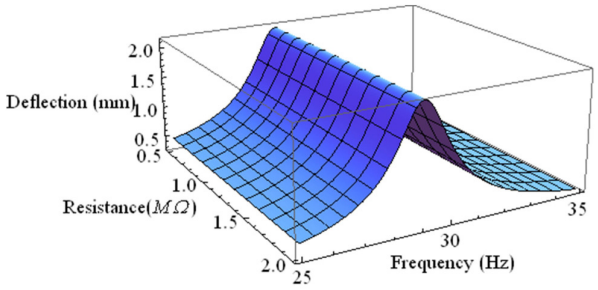

Figure 3. End mass displacement as a function of load resistance and the frequency of excitation for 0.5 g input.

Voltage frequency response function is portrayed in Figure 4 for different values of load resistances. It is to be noticed that the potential at resonance increases as the load is increased. The plot shows the voltage developed for three values of load resistance – 150 kΩ, 500 kΩ, and 1 MΩ. However, the power output has a maximum at the load resistance given by equation (18).

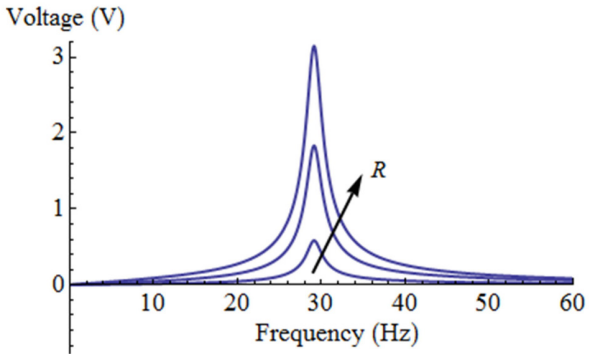

Figure 4. Voltage frequency response for three values of load resistance - 150 kΩ, 500 kΩ, and 1 MΩ for 0.5 g input.

In the selected configuration of the multi-layer harvester, the peak power occurs at 1.38 MΩ of load resistance. The simulated plot of power generated as a function of frequency and load resistance is depicted in Figure 5. It is to be noted that the optimum load given by equation (18) coincides with the load resistance corresponding to the maximum power depicted in Figure 5.

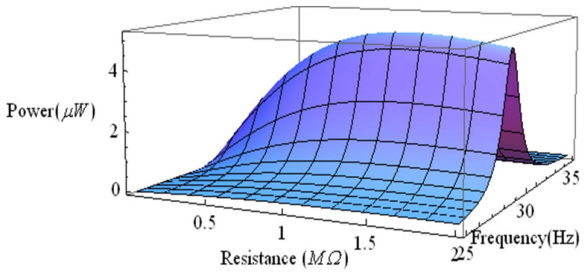

Figure 5. Simulation of the generated power with load resistance and frequency of vibration for the input excitation of 0.5 g.

Voltages developed by each layer of the multi-layer are experimentally measured for an input of 0.5 g at the beam resonance. The experimentally measured potential is compared with the predicted values in Figure 6.

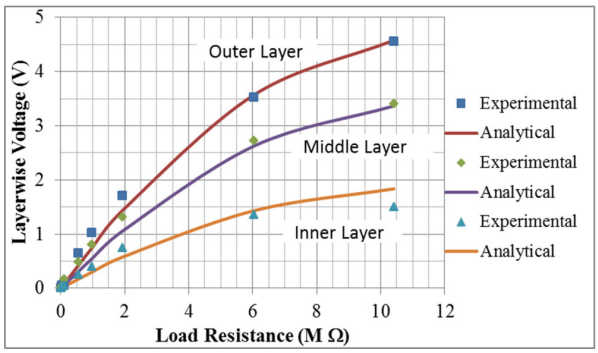

Figure 6. Layer-wise voltage measurements from a multi-layer harvester for 0.5 g input.

The fabricated harvester is subjected to three levels of input vibration 0.1, 0.2 and 0.5 g swept from 20 to 60Hz at 2 Oct/min and voltage is measured across several load resistances.

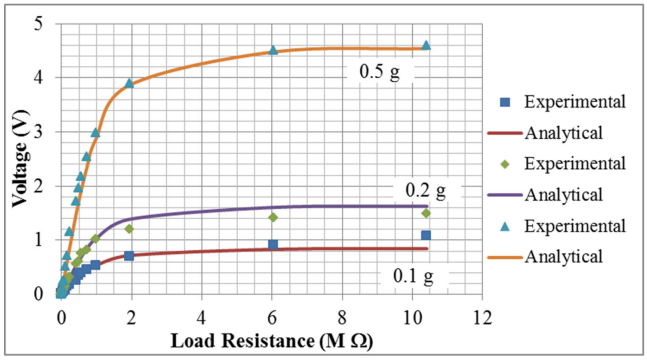

Figure 7. Experimental and analytical values of voltages from the 6 layered harvester at resonance across several load resistances for three different input levels of vibration – 0.1 g, 0.2 g and 0.5 g.

The voltage is measured at the device level combining all the layers for three different levels of input and is compared with the analytical values as shown in Figure 7. The measured voltage for 0.5 g input matches with the analytical value within 1% for several load resistances.

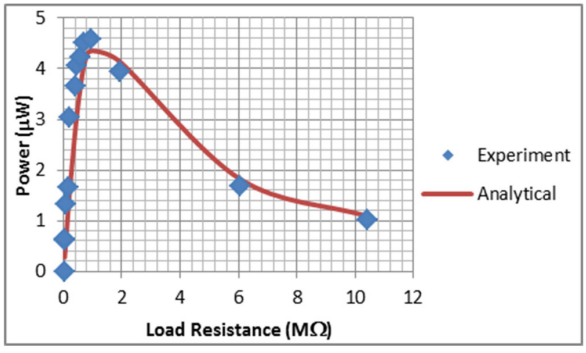

Figure 8. Experimental and analytical values of power from the 6 layered harvester at resonance across several load resistances for 0.5 g input vibration.

The power generated by the harvester as a function of load resistance is compared with the predicted values at resonance for 0.5 g input as plotted in Figure 8. It is evident from figures 5 and 8 that the maximum value of power for the selected configuration is 4.5μW and this corresponds to the optimum load resistance of 1.38 MΩ.

Following the methodology outlined for the multi-layer harvester, performance of the most ubiquitous configuration – the *bimorph* – is studied. Thickness of the copper substrate and length of the beam are 50 μm and 35 mm respectively resulting in beam resonance at 30Hz. The bimorph is excited by an input of 0.5 g at the harvesters resonance and the power measured is compared with the predicted values in Figure 9. It can be noticed from the plot that maximum power generation occurs at 3.3 MΩ which is equal to that calculated from equation (18).

Comparison of figures 8 and 9 indicates that peak power transfer from the multi-layer harvester occurs at a lower load resistance than that from a bimorph owing to the increase in G and C_p.

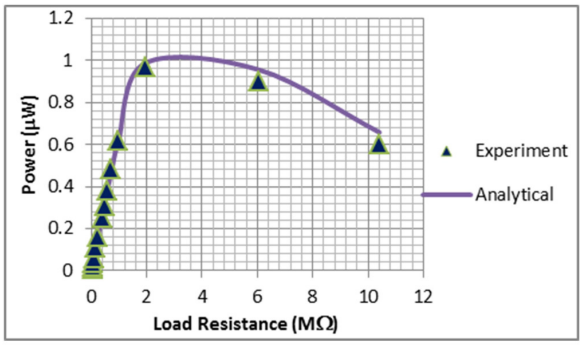

Figure 9. Experimental and analytical values of power from bimorph at resonance across several load resistances for 0.5 g input vibration.

Furthermore, it is noticed that in the parlance of power per unit volume of the piezoelectric material, multilayer harvesters stand at 58 μW/cm^3 while the bimorph configuration is at 28 μW/cm^3 when operated at their respective optimal load resistances. However, power density in case of the bimorph decreases further at lower load resistances.

5. CONCLUSIONS

The present work presents the performance analysis of a multi-layer harvester. Salient performance parameters associated with the multi-layer harvesters are the improved electro-structural coupling coefficient and the total capacitance. Current work also includes the exact analysis of the stepped multi-layer piezoelectric beam with no approximations in beam modeling.

Dependence of the power on load resistance is verified in multi-layer and bimorph types of harvesters made with PVDF material. The predicted optimum load resistance in both cases is corroborated experimentally. Furthermore, it is verified that under similar operating conditions, the power generated by a multi-layer harvester is higher than that of the bimorph for a given volume of the piezoelectric material, demonstrating higher power densities inducible by design. The effectiveness of the harvester is determined by the power density normalized to the excitation acceleration. The normalized power density for PVDF multi-layer harvester is 232 μW/cm^3/g^2 and that for a PVDF bimorph is 98 μW/cm^3/g^2. This indicates considerable improvement in the generated power by the multi-layer configuration over bimorph harvesters, for a given volume of piezoelectric material and the input levels of vibration. The ambient energy levels are innately low and hence, it becomes crucial to improve the performance of the harvesters. For better effectiveness, it is recommended to harvest energy from vibrations using multi-layer beam configuration. Low cost and ease of fabrication associated with PVDF film make it ideal to implement multi-layer arrangement which is superior in performance to the bimorph configuration.

ACKNOWLEDGMENT

This work is partially supported by NPMASS grant and the facilities created by NPMASS projects at CeNSE, I.I.Sc. S. R. acknowledges the guidance given by Prof. Navakant Bhat in the examination of multi-layer harvester experimental results.

REFERENCES

[1] S. P. Beeby, R. N. Torah, M. J. Tudor, P. Glynne-Jones, T. O'Donnell, C. R. Saha, S. Roy, 2007 A micro electromagnetic generator for vibration energy harvesting, *J. Micromech. Microeng*, 17, pp 1257-1265.

[2] P. D. Mitcheson, E. K. Reilly, P. K. Wright, E. M. Yeatman, 2006, Transduction mechanisms and power density for MEMS inertial energy scavengers, *Proc. Power MEMS.*

[3] Shad Roundy, Paul K. Wright, Jan Rabaey, 2003, A Study of low level vibrations as a power source for wireless sensor nodes, *Computer Communications* 26, pp. 1131-1144.

[4] Micka¨el Lallart and Daniel J. Inman, 2010, Low-Cost Integrable Tuning-Free Converter for Piezoelectric Energy Harvesting Optimization, *IEEE transactions on power electronics*, Vol. 25, no. 7.

[5] A. D. T. Elliott and P. D. Mitcheson, September 2012, Implementation of a single supply pre-biasing circuit for piezoelectric energy harvesters, *EuroSensors 2012.*

[6] S. Roundy and P. K. Wright, 2004, A piezoelectric vibration based generator for wireless electronics, *Smart Mater Struct.* **13** 1131–42.

[7] T. Eggborn, 2003, Analytical Models to Predict Power Harvesting with Piezoelectric Materials, *M.S. Thesis*, Virginia Polytechnic Institute and State University.

[8] R. Shukla, L. C. Lim, P. Gandhi, 2009, Piezoelectric single crystal power generator for low frequency vibrating machines and structures, *18th IEEE International Symposium on the Applications of Ferroelectrics, ISAF 2009.*

[9] H. A. Sodano, G. Park and D. J. Inman, 2004, Estimation of electric charge output for piezoelectric energy harvesting, *J. Strain* **40** 49–58.

[10] R. G. Ballas, 2007, Piezoelectric Multilayer Beam Bending Actuators - Static and Dynamic Behavior and Aspects of Sensor Integration, *Springer* pp 54-55.